Available online at www.sciencedirect.com

ScienceDirect

Defence Technology 12 (2016) 401–418

www.elsevier.com/locate/dt

An overview on importance, synthetic strategies and studies of 2,4,6,8,10,12-hexanitro-2,4,6,8,10,12-hexaazaisowurtzitane (HNIW)

J. VENKATA VISWANATH [a,b], K.J. VENUGOPAL [a], N.V. SRINIVASA RAO [b], A. VENKATARAMAN [a,c,*]

[a] *Materials Chemistry Laboratory, Department of Materials Science, Gulbarga University, Kalaburagi, 585106 Karnataka, India*
[b] *R&D Center, Premier Explosive Limited, P.O. Peddakandukur-508286, Yadagirigutta Mandal, Nalgonda District, Telangana, India*
[c] *Department of Chemistry, Gulbarga University, Kalaburagi, 585106 Karnataka, India*

Received 15 December 2015; revised 18 May 2016; accepted 24 May 2016

Available online 30 May 2016

Abstract

2,4,6,8,10,12-Hexanitro-2,4,6,8,10,12-hexaazaisowurtzitane (HNIW), commonly called as CL-20, is a high energy and high density material of keen interest to both commercial and scientific worlds due to its greater insensitivity (reduced sensitivity) along with a positive high heat of formation, which is due to the azanitro groups attached to the skeleton of HNIW and its highly strained cage structure. It plays a remarkable role in modification and replacement of most of the propellant (gun and rocket) preparations. In this report we present the comparative strategies involved in the syntheses of HNIW with respect to economical and environmental aspects. Various methods reported in the literature on the purification of the crude HNIW (α-HNIW) to obtain ε-form of HNIW (high dense/more potential) are consolidated. Understanding of the structure, morphology, energetics, thermal behavior and their modification to meet the applicability (decreased impact sensitivity) determines the industrial application of HNIW. A compilation of the available literature on the aforementioned characteristic properties for obtaining a value added ε-HNIW is discussed here. This overview also reports the literature available on newer forms of HNIW including derivatives and cocrystals, which increase the performance of HNIW.

Keywords: High energetic materials; Synthetic strategies; Caged nitramine; Thermal stability; Impact sensitivity

1. Introduction

The search for latest high energetic and high density material is an area of intense interest in military and industrial applications [1–4]. Defense services have been challenged to replace the high sensitive, high energy propellants with materials that have similar energy but are less-sensitive, and can perform under a wide range of temperatures. HNIW is found to be more eco-friendly as well as reduces a missile's plume signature without encountering combustion stability problems [5,6]. HNIW is also found to be one of the most powerful non-nuclear explosive materials and shows great scientific advances in future weapon systems [7]. HNIW is superior in comparison to other high energetic explosive materials such as HMX, RDX, PETN, etc., with respect to density, velocity of detonation, detonation pressure and enthalpy of formation. A comparison of these is notified in Table 1. HNIW has high density ($\rho > 2$ g/cm^3), a positive heat of formation ($\Delta H_f = 454$ kJ/mol) [9], high detonation velocity (9.4 km/S) and an optimum oxygen balance (−11.0) as well as an optimum detonation pressure (420 kbar) [8]. HNIW also has a higher oxidizer-to-fuel ratio. With the aforementioned prominent parameters, HNIW attracts the attention of propellant and explosive manufacturers [14,15]. The reasons for higher detonation pressure of HNIW are due to the presence of —NO_2 groups in the FMR and SMR [16]. The greater energetic content of caged polycyclic nitramine [17] and its high molecular density over the remaining cyclic nitramine explosives like HMX and RDX make it a better candidate for propellant applications [10,11]. Based on the study of cylinder expansion and tantalum plate acceleration experiments, HNIW was found to be approximately 14% greater than HMX in its performance [18]. HNIW exists in four stable polymorphs with different crystal structures, viz., α-, β-, γ- and ε-forms. The ε-form among the remaining is the least

Peer review under responsibility of China Ordnance Society.
* Corresponding author. Tel.: +919880801017.
E-mail address: raman_chem@rediffmail.com (A. VENKATARAMAN).

http://dx.doi.org/10.1016/j.dt.2016.05.002

Nomenclature

ADN	ammonium dinitramide
CAN	cerium (IV) ammonium nitrate
CI	chemical ionization
CID	collision-induced dissociation
CRSE	conventional ring strain energy
D	dihedral angle of SMR taken from (C6,C5,N11,C9) [13]
D′	dihedral angle of SMR taken from (C5,C6,N12,C10) [13]
DFT	density functional theory
DFTHP	1,4-diformyl-2,3,5,6-tetrahydroxypiperazine
DMSO–THF	dimethyl sulfoxide–tetrahydrofuran
DMF	dimethylformamide
DNOIW	dinitrosohexaazaisowurtzitane
DOA	dioctyl adipate
EECC	energetic–energetic cocrystal
EI	electron impact
FMR	five member ring
GAP	glycidyl azide polyol
HAIW	hexaacetylhexaazaisowurtzitane.
HallylIW	hexaallylhexaazaisowurtzitane
HBIW	hexabenzylhexaazaisowurtzitane
HDI	hexamethylenediisocyanate
HEM	high energetic materials
HMX	octahydro-1,3,5,7-tetranitro-1,3,5,7-tetrazocine
HNF	hydrazinium nitroformate
HNIW	hexanitrohexaazaisowurtzitane
HPIW	hexa(1-propyl) hexaazaisowurtzitane
HSIW	hexasulfamatohexaazaisowurtzitane
HTPB	hydroxy terminated polybutadiene
LSHEM	low sensitive high energy material
MIKE	metastable mass analyzed ion kinetic energy
MSDS	Material Safety Data Sheet
N_{aza}	aza nitrogen
N_{nitro}	nitro nitrogen
NC	nitrocellulose
N_2O_4	dinitrogen tetroxide
$NOBF_4$	nitrosonium tetrafluoroborate
NO_2BF_4	nitronium tetrafluoroborate
NMR	nuclear magnetic resonance
PAIW	pentaacetylhexaazaisowurtzitane
PAFIW	pentaacetylformylhexaazaisowurtzitane
PCNA	polycyclonitramines
PETN	pentaerythritoltetranitrate
PolyGLYN	poly(glycidyl nitrate)
PolyNIMMO	poly(3-nitratomethyl-3-methyloxetane)
RDX	1,3,5-trinitroperhydro-1,3,5-triazine
SAXS	small angle X-ray scattering
SMR	six member ring
TADAIW	tetraacetyldiamineisowurtzitane [25]
TAIW	tetraacetylhexaazaisowurtzitane [40]
TADBIW	tetraacetyldibenzylhexaazaisourtzitane
TADFIW	diformyltetraacetylhexaazaisowurtzitane
TADNIW	tetraacetyldinitrohexaazaisowurtzitane
t-BuOK	potassium t-butoxide
TATBIW	triacetyltribenzylhexaazaisowurtzitane
TATFIW	triaacetyltriformylhexaazaisowurtzitane
TDI	toluene 2,4-isocyanate
THMNM	tris(hydroxymethyl)nitromethane
TNT	trinitrotoluene

sensitive and possesses the highest density (2.04 g/cm^3) and detonation velocity. The physical parameters of the ε-form of HNIW are given in Table 1 [19]. Murray et al. [20] discussed the importance of charge redistribution in the cage of HNIW based on the triggered linkage molecules (N—NO_2). Based on physical parameters, the ε-form of HNIW is considered to be the best suitable explosive material among all its polymorphs. The ε-form is prepared from the raw HNIW employing any of these techniques – solvent evaporation or precipitation method employing solvent and non-solvent (antisolvent). The recent report on the functionalization of ε-HNIW using reduced graphene oxide and Estane shows further improvement in the properties of pure ε-HNIW in terms of mechanical stability, sensitivity and density [21,22].

Table 1
Physicochemical properties of some important high energy materials.

Sl. No.	Energetic materials	ΔH_f/(kJ·mol^{-1})	OB/%	Density ρ/(kg·m^{-3})	Detonation velocity/(km·s^{-1})	References
1	HNIW	+454	−11.0	2040	9.38	[8]
2	HMX	+76	−22.0	1910	9.100	[9–11]
3	RDX	+63	−22.0	1820	8.750	[9–11]
4	ADN	−135	+26.0	1808	6.3	[12]
5	AP	−298	+35.0	1950	–	[12]
6	PETN	−540	−10.1	1770	8.400	[9,13]
7	TNT	−26	−74	1654	6.900	[9,13]

ΔH_f kJ/mole = heat of formation kilojoules per mole.
OB/ % = oxygen balance in %.
Density ρ/kg/m^3 = kilogram per meter cube.
Detonation velocity km/s = kilometers per second.

A major scientific breakthrough came when a China Lake researcher Nielsen synthesized the energetic solid HNIW [23]. The scale up method for the synthesis of HNIW was explained by Gore [24] and Latypov et al. [25]. The cage structure of HBIW is unstable due to oxidation via loss of two electrons by degradation mechanism that was reported by Guan et al. [26]. The sources of strain and energy of the different polymorphs of the HNIW are theoretically explained by Zhou et al. employing DFT [17]. The high density of ε-polymorph of HNIW is attributed to the greater stability toward shock and gives higher rate of detonation [27]. Optimization of the process parameters for the synthesis of HNIW in the required particle size through the intermediate TAIW is explained by Mandal et al. [13]. However, it has high impact and friction sensitivity close to those of PETN [12]. Controlling the crystal density and lowering the mechanical sensitivity of HNIW have attracted a great deal of attention in order to produce insensitive HEMs [28,29].

Although HNIW is reported vastly in the literature as various synthetic strategies, reduced sensitivity, modification of morphology and so on, however, a comprehensive understanding of all the required parameters is sparingly given [9,30–32]. This overview is aimed at presenting the holistic approach on synthetic strategies to obtain HNIW with reduced sensitivity, high velocity of detonation, etc.

Synthesis of the HNIW is considered to be one of the most complicated procedures. A lot of papers have shown different procedures involving multiple steps and methodologies for the synthesis. Here we discuss some of the reported synthetic procedures and some important strategies, along with possible reaction pathways and reaction schemes. Discussion on the synthetic strategies and higher cost involved when palladium (Pd) based catalysts are used, and the alternate routes to overcome that problem are presented in detail. Conclusions are also drawn from these studies to choose the most possible synthetic strategy for scale up, which will benefit the researchers in choosing a modified strategy.

This overview covers the literature on the characteristics of HNIW like thermal behavior/transformations [33] and FTIR, energetics and modification of impact sensitivity to meet its applicability. This overview also reports the literature on derivatives [34] and cocrystals [35,36a,b,37] formed from HNIW with induced characteristics to meet the needs.

2. Report oversurvey on syntheses

Classical method for synthesis of HNIW requires benzylamine and glyoxal as precursors. The usage of benzylamine precursor has limitations, including unsafe synthesis of benzylamine [30] and the debenzylation step that follows that [9]. Different types of catalysts ranging from high cost (Pd/C) to the more attentive CAN [29] were employed in the debenzylation process. Nitration of the different debenzylated products is also understood to employ different nitrating agents.

The above procedure was replaced by a versatile method for synthesis of HNIW to eliminate hazardous benzylamine precursor and the costly debenzylation process. Here the precursors used were allylamine and glyoxal, which were used to form an intermediate HallylIW. On catalytic action, the HallyIW is converted to HPIW, which is then easily nitrated with normal nitrating agents like a mixture of HNO_3 and H_2SO_4. In this process the yield was 82%. The allylamine precursor preparation involves easy and economically appreciable process when compared to that of benzylamine precursor. The product obtained in this procedure has higher efficiency [30,31].

The condensation of glyoxal with sulfamate derivatives produces HNIW in a much economical way. The synthesis has an advantage of easy nitration of protecting group (sulfamate derivative). This two-step method of synthesis of HNIW does not encounter the problems of hazardous precursors and heavy metal catalysts. It neither needs laborious work nor much time to synthesize. The glance on obtaining good yield of required intermediate HSIW out of the precursors and nitration of that intermediate to get pure HNIW is the futuristic work in the field of PCNA [38,39].

The procedure to synthesize HNIW without benzylamine as a starting material was proposed. This new procedure involves 1,4-diformyl-2,3,5,6-tetrahydroxypiperazine (DFTHP) and 1,1,2,2-tetraamidoethane derivatives as precursors. In this route a strained cage structure of TADFIW is directly obtained, skipping expensive and time consuming debenzylation reaction. The nitration of TADFIW gives yield up to 98% of HNIW [40]. The advantage of this process is that we can regenerate the acetyl protecting group that is introduced at the starting step, after nitrolysis.

3. Synthesis procedures

The three different procedures mentioned earlier along with a proposed procedure and purification method are discussed in detail in the following section. Procedure 1 involved benzylamine as a precursor and is explained through seven different synthesis strategies along with the reaction mechanisms involved. In Procedure 2, allylamine and glyoxal are mentioned as the precursors, and in Procedure 3, glyoxal and metal sulfamate are the precursors. In the proposed procedure DFTHP and 1,1,2,2-teraamindoethane derivatives are the precursors. The reaction mechanisms reported are compiled here.

3.1. Procedure 1

The starting material for the synthesis of HNIW was benzylamine. Benzylamine synthesis involved chlorination of toluene to form benzylchloride [41] followed by ammonia treatment to form benzylamine. Hence HNIW production faces all the chlorine manufacturing industry problems such as long time toxicity of organochlorine by-products and contamination due to mercury which is involved in the industrial chlor-alkali procedure to generate chlorine [30]. Also benzylamine itself is an environmentally unwanted starting material as per its MSDS.

Formation of cage structure is the key step in the synthesis of HNIW through benzylamine. The strain energy that is the prime criterion for high heat of detonation is obtained through the cage formation. The cage structure of HBIW is obtained by the end to end condensation of benzylamine and glyoxal precursors

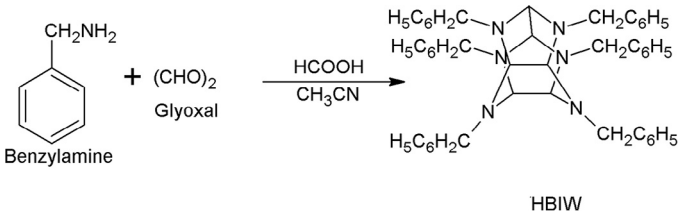

Fig. 1. Synthesis of HBIW.

as shown in Fig. 1. The synthesis of HBIW involves acid catalyzed condensation of benzylamine with aqueous glyoxal (40%). This procedure yields around 80% of HBIW having 95% purity. Syntheses of HBIW were carried out by a variety of acid catalysts, such as formic acid, acetic acid and sulfuric acid. The reaction was fast and goes to completion with formic acid in acetonitrile as the acid catalyst and when the reaction combination was maintained at pH 9.5. The initial attempt to synthesize HBIW from benzylamine and glyoxal precursors was made by Nielsen et al. [42]. Conversion of HBIW to HNIW poses a major challenge. Direct nitration of HBIW to form HNIW by nitrolysis will be unsuccessful because of competing nitration of phenyl rings [1], which made the scientists choose hydrogenation prior to nitrolysis. With HBIW itself being unstable, hydrogenolysis in the absence of the reactive acetylating agent leads to the collapse of the cage structure [9]. The next step in HNIW synthesis was debenzylation of HBIW. Reductive hydrogenolysis method is extensively used to debenzylate HBIW [11]. The acetyldebenzylation of HBIW leads to the formation of intermediate polyacetylpolybenzyl derivatives [1]. The replacement of benzyl groups with nitro groups through acetyldebenzylation may be successful using various catalysts and nitrating agents.

The debenzylation followed by the nitration of HBIW to HNIW is a crucial step in synthesizing HNIW. Here we discuss different strategies adopted in the literature for the same.

3.1.1. Strategy 1

In the phenomenon of reductive hydrogenolysis (acetyl debenzylation) of HBIW, one of the intermediate products (polyacetylpolybenzyl derivative) was TADBIW. Best yields were obtained by catalytic hydrogenolysis using palladium hydroxide on carbon with acetic anhydride solvent along with the acid promoter like HBr under atmospheric pressure of hydrogen. The yield of TADBIW obtained in this procedure is around 60–65% [1]. Four benzyl groups are changed into four acetyl groups as a result of catalytic hydrogenolysis, while benzyl groups at 4- and 10-positions at the SMR of HBIW are immovable. The detailed reaction pathway for the synthesis of TADBIW and its nitration to HNIW is explained by Yuxiang et al. [43] with a yield around 71.7% of HNIW. The chemical representation of the synthesis of HNIW through TADBIW is given in Fig. 2. Bescond et al. [44] have reported the synthesis of α-HNIW from TADBIW by nitrating it with N_2O_4 and H_2SO_4/HNO_3 mixture. The yield of around 97% is obtained with a purity of >95%.

TATBIW is one of the intermediates obtained after reductive hydrogenolysis of HBIW. The acetyl debenzylation of HBIW with acetic anhydride, DMF, bromobenzene and $Pd(OH)_2/C$ catalyst gives TATBIW [45]. The reaction is shown in Fig. 3. The yield of TATBIW obtained in this procedure is around 55%. The authors [45] have presumed to synthesize HNIW by nitration of TATBIW. Li et al. [46] have synthesized TATFIW from TATBIW.

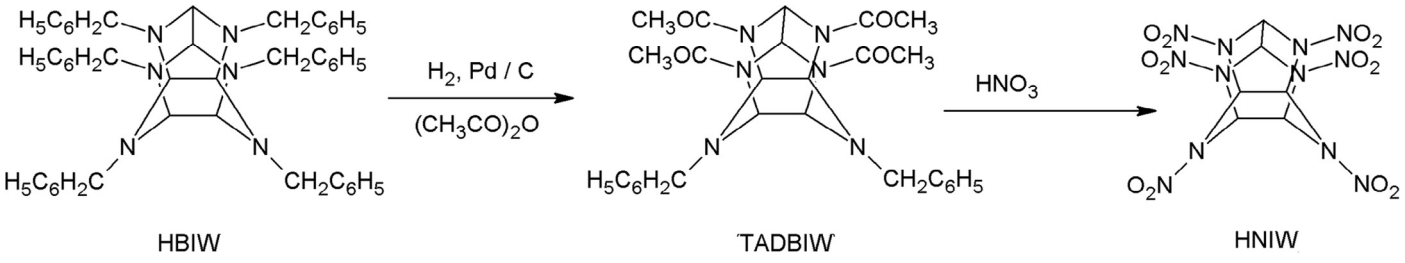

Fig. 2. Synthesis of HNIW from TADBIW.

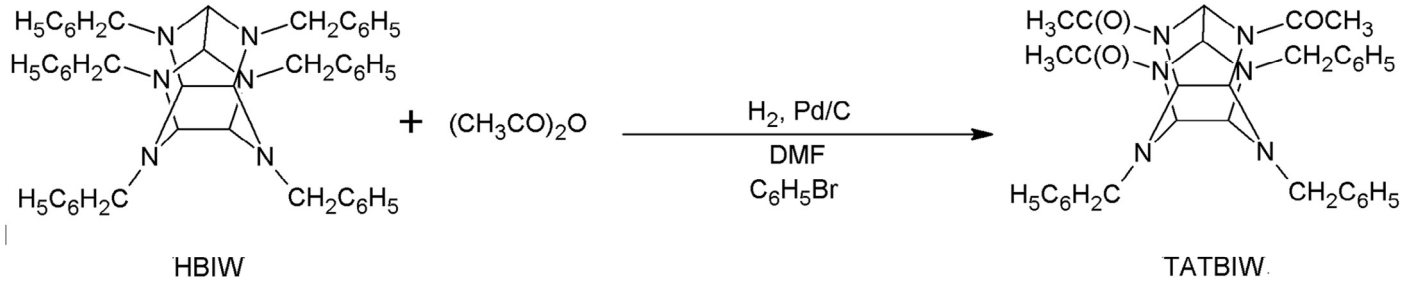

Fig. 3. Synthesis of TATBIW.

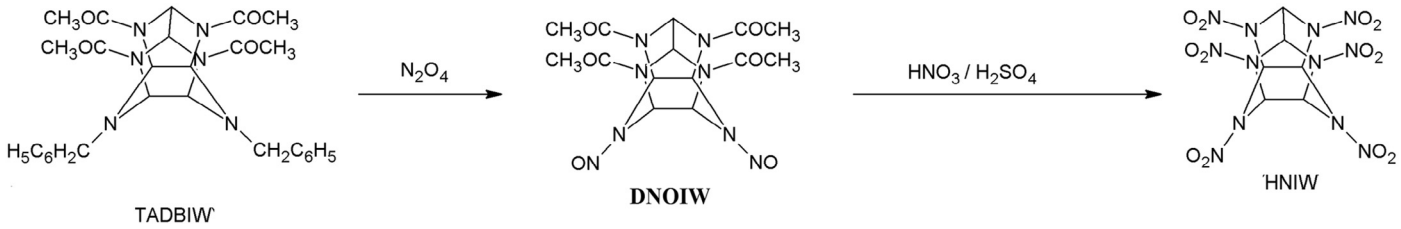

Fig. 4. Synthesis of HNIW through nitrosation of TADBIW.

3.1.2. Strategy 2

The nitrosation of TADBIW to DNOIW and further nitration to HNIW was established by Nielsen [47]. The process is expensive as it involved $Pd(OH)_2/C$ catalyst and BF_4 based nitrating agents. Wardle and Edwards [48] and Latypov et al. [25] had made some successful attempts to overcome this problem. The nitrosation of TADBIW to DNOIW using N_2O_4 and further nitration of the DNOIW to HNIW using the mixture of HNO_3 and H_2SO_4 was proposed. The yield obtained in this procedure was around 95.1%. The product formed in this procedure was superior to the one obtained by the reported one pot method suggested by Latypov et al. [25]. The mechanism of synthesis is given in Fig. 4.

3.1.3. Strategy 3

Hydrogenation of HBIW with $Pd(OAc)_2$ catalyst in the presence of formic acid as a solvent yields TADFIW as per Wardle and Edwards [49]. Batches were made to optimize the essentiality of the palladium catalyst [9] as an economy measure. Rao et al. [50] reported the nitration of TADFIW with 98% of concentrated HNO_3 at around 125 °C to produce 90–97% yield of HNIW as shown in Fig. 5. Formation of formylated impurities is a drawback of this method. Shaohua et al. [51] have reported the synthesis of ε-HNIW employing one pot method by nitration of TADFIW using HNO_3. The yield reported is 91.4%.

3.1.4. Strategy 4

This strategy illustrates the synthesis of HNIW from TADBIW through TADNIW. TADNIW was synthesized through nitration of TADBIW with the mixture of $NOBF_4$ and NO_2BF_4, which was followed by nitration with NO_2BF_4 to give HNIW [52] as shown in Fig. 6. The protecting group (acetyl group), which is used to replace the benzyl group, should be readily replaceable by the nitro group. The yield obtained through this procedure was around 90%.

One-pot synthesis reported by Wang et al. [53] was a modified approach to HNIW synthesis from TADBIW through TADNIW in which the yield attained was around 82% and purity attained was 98%.

3.1.5. Strategy 5

Kawabe et al. [54] claimed that the mixed acid nitration of TADAIW at 60 °C for 24 hours yielded 98% of HNIW. Sanderson et al. [55] obtained HNIW from mixed acid nitration of TADAIW at 85 °C in which the conversion was 99%, and the reaction time was less than ten minutes. The process followed by Kawabe et al. [54] and Sanderson et al. [55] is shown in Fig. 7. Attempts were made to optimize the synthesis of HNIW through nitration of TADAIW using 95–99% HNO_3 [56]. The yield reported through this optimized procedure is around 85%.

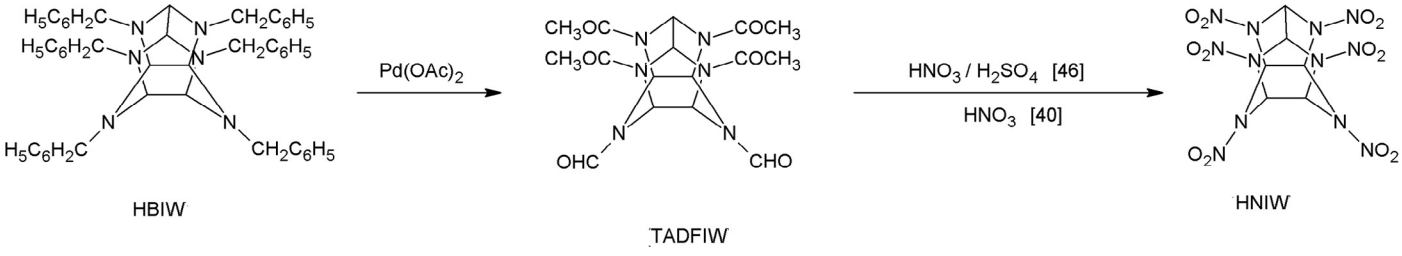

Fig. 5. Synthesis of HNIW through TADFIW.

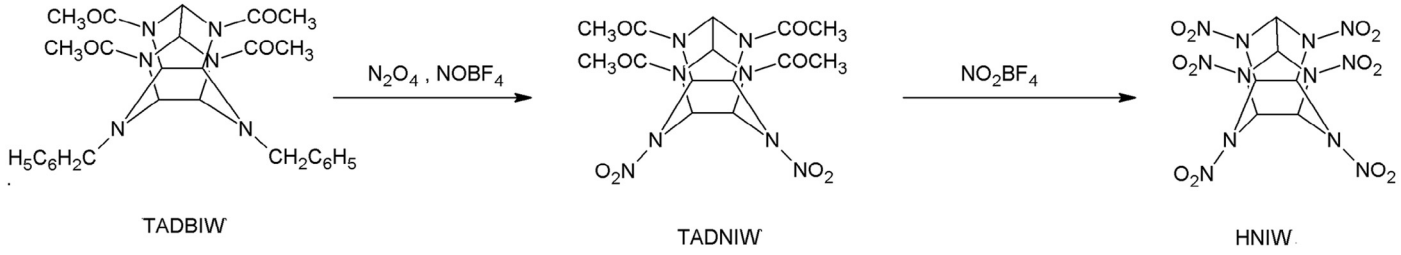

Fig. 6. Synthesis of HNIW through TADNIW.

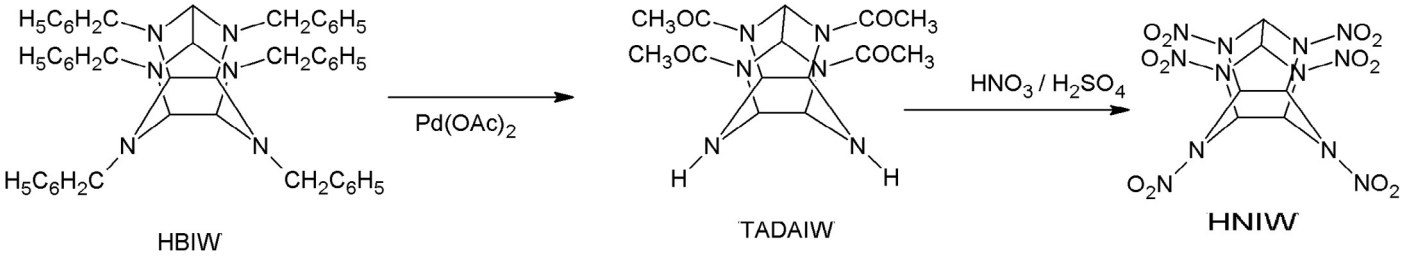

Fig. 7. Synthesis of HNIW through TADAIW.

3.1.6. Strategy 6

The debenzylation procedure of HBIW also formed TAIW or HAIW. The existing procedures to synthesize these products were established by Kodama [57] and Gore et al. [29] respectively. The reaction is given in Fig. 8. The nitration procedures were successfully explained by Hamilton et al. [58] and Gore et al. [29]. But the process of avoiding the polluting effect of these procedures was established by Bayat and Mokhtari [59]. The product HNIW is isolated in the hydrated α-form after drying to a constant weight at 40 °C. The procedure adopted was nitrating TAIW by HNO_3/N_2O_4 to form HNIW. The product yield obtained in this process was around 97%. The reaction is given in Fig. 9. The process adopted by Gore et al. [29] to nitrate TAIW to HNIW was optimized by Mandal et al. [13]. The schematic representation is given in Fig. 10. The process of nitrating HAIW to obtain HNIW was given by Gore et al. [29].

3.1.7. Strategy 7

Nitration of TAIW, TADFIW and HAIW has some drawbacks, such as TAIW cannot be isolated easily, firing problem during TADFIW handling and HCl gas evolvement when using HAIW [60]. To overcome this problem, Chung et al. [60] have proposed a better procedure in the conversion of TAIW to PAIW and PAFIW. The PAIW and PAFIW are reported to be nitrated with a mixture of HNO_3/H_2SO_4 to yield HNIW of 97% and 96% respectively. The probable mechanism of this reaction is given in Fig. 11.

3.2. Procedure 2

To overcome the problems in the debenzylation procedure, an alternative route to synthesize HNIW had come to the spotlight with the precursors such as allylamine and glyoxal to form

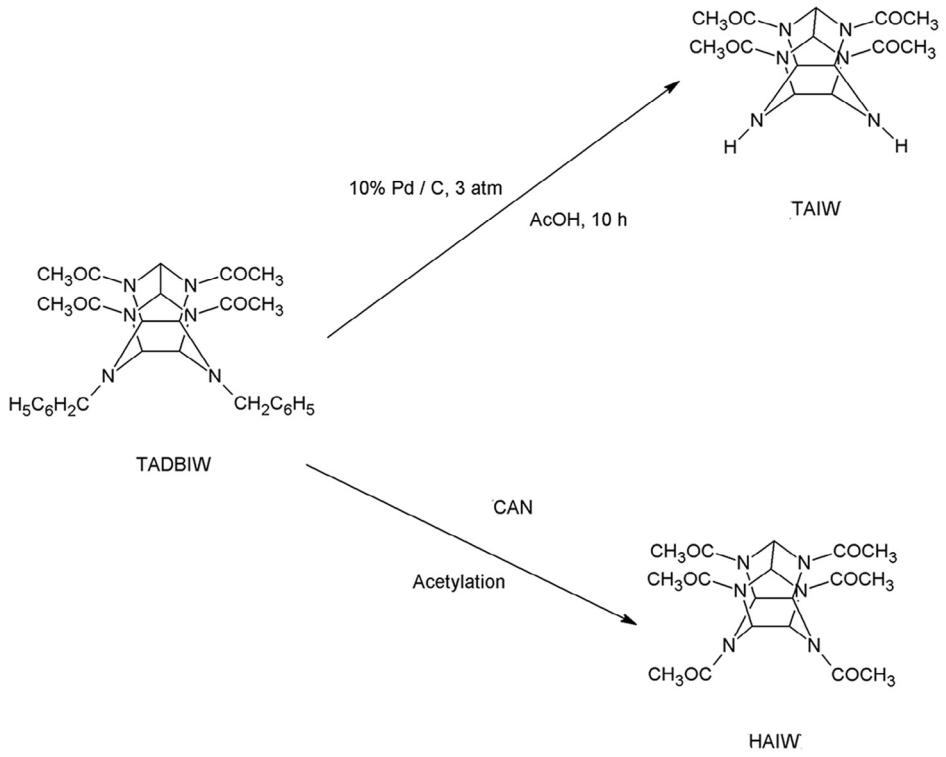

Fig. 8. Synthesis of TAIW/HAIW through TADBIW.

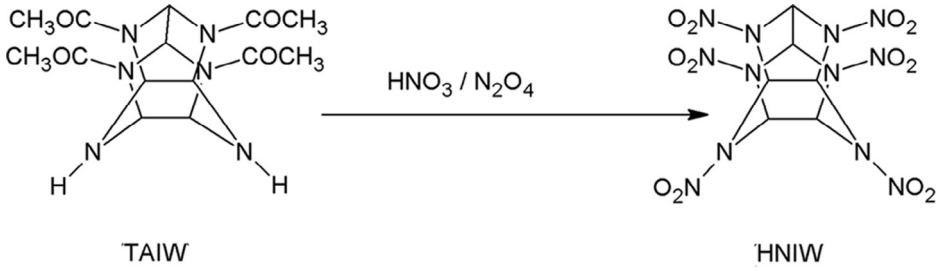

Fig. 9. Synthesis of HNIW through TAIW.

HAllylIW. HAllylIW reacts with *t*-BuOK (catalyst) DMSO–THF to form HPIW, which is further nitrated to HNIW using simple nitrating agents like HNO_3 acid catalyst [31]. It has also been reported that HPIW on photo oxygenation and further nitrolysis in the presence of Nafion NR 50 bead as a strong Bronsted acid catalyst yields efficient product [30]. The possible reaction pathway is shown in Fig. 12, and the scheme for synthesis is shown in Fig. 15(b).

3.3. Procedure 3

Sysolyatin et al. [38,39] had made a significant contribution in synthesizing HNIW in a resourceful method that is devoid of benzylamine precursor. An attempt was made for the formation of polycyclic nitramine cage through the condensation of glyoxal and metal sulfamates. A series of intermediate products were formed depending on the reactants' ratio and reaction conditions. Among the formed intermediates HSIW derivative can be directly nitrated to HNIW using HNO_3. The choice of protecting group was sulfamate derivatives as they can be easily nitrated. The reactions have been shown in Fig. 13 and the scheme for synthesis is shown in Fig. 15(c). There are attempts like the above procedure to synthesize HNIW in two steps without involving hazardous, costly precursors or heavy metal, attention drawing catalysts and also time consuming laborious steps.

3.4. Proposed procedure

Chapman et al. [30] had proposed an interesting two-step synthesis of HNIW without benzylamine. This procedure begins with the precursors such as DFTHP and various 1,1,2,2-tetraamidoethane derivatives; among the derivatives, tetraacetamidoethane ($R = R' = CH_3$) is mostly employed for its low cost among all acetamide starting materials. A single bimolecular condensation of these two reactants under appropriate conditions may produce the hexaazaisowurtzitane cage (TADFIW approximately), which reacts with ammonium nitrate and HNO_3 acid mixture [40] to form HNIW with 98% yield. The reaction pathway is shown in Fig. 14, and the synthetic scheme is shown in Fig. 15(d). The referred advantage in this method is that the acetyl protecting group that is introduced in the earlier stage is easily regenerated after nitrolysis. Chapman et al. had reported the procedure was unsuccessful thus far [30].

3.5. Conversion of α-HNIW to ε-HNIW

The purification of the α-HNIW is explained by Bescond et al. [44] by two different methods, viz., mixing method and seeding methods. The authors have succeeded in obtaining ε-HNIW with different particle sizes. The authors have used different seeding media (toluene based) in purification of α-HNIW to get ε-HNIW. The pure HNIW may be obtained by adding *n*-heptane anti solvent to the ethyl acetate solution of crude HNIW. The precipitate of pure ε-HNIW is then filtered and air-dried. The report on recrystallization of ε-HNIW from α-HNIW (obtained from Premier Explosives Limited, India) was provided by Ghosh et al. [61] through solvent evaporation method (with and without ultrasound) and precipitation method. The yield (ε-HNIW) reported was around 85–90% with a chemical purity of 98%. The procedures to obtain pure ε-HNIW from α-HNIW and conversation of ε-HNIW to reduced sensitive-ε-HNIW (RS-ε-HNIW) have been compiled in the subhead "Impact sensitivity and its modification" and are discussed below.

The above procedures and the synthetic strategies along with citations are categorized and given in Table 2.

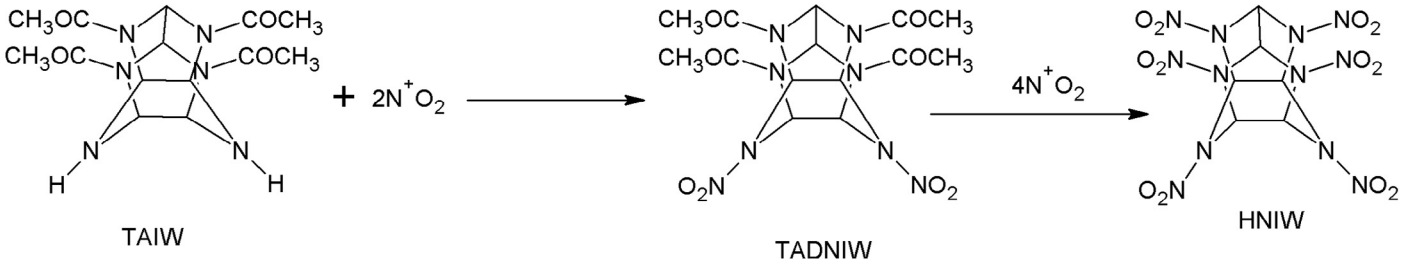

Fig. 10. Synthesis of HNIW through nitration of TAIW and TADNIW.

Table 2
Comparison on the methods of synthesis of HNIW.

Sl. No.	Methods	Routes	Reactants	References	Benefits/Drawback
1	Procedure 1 Nitrolysis	Strategy 1	Benzylamine, glyoxal, acetic anhydride, DMF, bromobenzene and Pd $(OH)_2$/C	[1,43,45]	Yield 12.8–40% Yield 71.7% Yield 55% Complicate reaction, long procedure, time consumable, high cost and low yield
		Strategy 2	$Pd(OH)_2$/C catalyst and BF_4^-	[25,47,48]	Yield 95.1%
		Strategy 3	$Pd(OH)_2$/C catalyst and formic acid	[9,49,50]	75% yield
		Strategy 4	$NOBF_4$ and NO_2BF_4	[52,53]	Yield of 90–96% and >95% pure
		Strategy 5 One-pot synthesis Mixed acid nitration	$Pd(OH)_2$/C, HNO_3, H_2SO_4	[54,55]	Yield up to 82% and purity up to 98% 99% conversion within ten minutes
		Strategy 6 Nitration by various nitrating agents	HNO_3/N_2O_4	[13,24,29,57–59]	Lengthy procedure with moderate yield Yield 98%
		Strategy 7 Nitrating PAIW/PAFIW	TAIW, HNO_3/H_2SO_4	[60]	Problems aroused with TAIW, TADFIW and HAIW are dealt here. Yield 97% with PAIW, 96% with PAFIW
2	Procedure 2 (i) HPIW method (ii) Benzyl amine free synthesis	Allyl amine, formic acid, glyoxal, t-BuOK (cat) DMSO–THF, HNO_3 acid catalyst, Nafion NR 50 bead		[30,31]	Yield 98% Low cost and high yield Yield 80%–98% Time consumable (31 h)
3	Procedure 3 Metal sulfamate method	Glyoxal and metal sulfamate, nitric acid		[38,39]	Without involving hazardous, costly precursors or heavy metal, attention drawing catalysts and also time consuming laborious steps
4	Proposed procedure	Glyoxal, 1,4-Diformyl-2,3,5,6-tetrahydroxypiperazine, 1,1,2,2-tetraamidoethane derivatives, TADF, ammonium nitrate, HNO_3 acid mixture		[30,40]	Yield 80% Yield 98% Low cost and high yield
5	One-pot method directly from TADFIW	TADFIW and nitric acid, hydrolysis–nitration mechanism carried out at 85 °C–95 °C for 6 h		[51]	91.4% yield and 99.56% pure
6	Normal micro emulsion based nonionic surfactant	n-Butyl acetate, ethyl acetate, Tween80, 2-propanol		[56]	HNIW nanoparticles be synthesized through this process
7	The reaction parameters were optimized in this method	TADAIW nitration by 95–99% nitric acid		[62]	Highly economical with 85% of yield

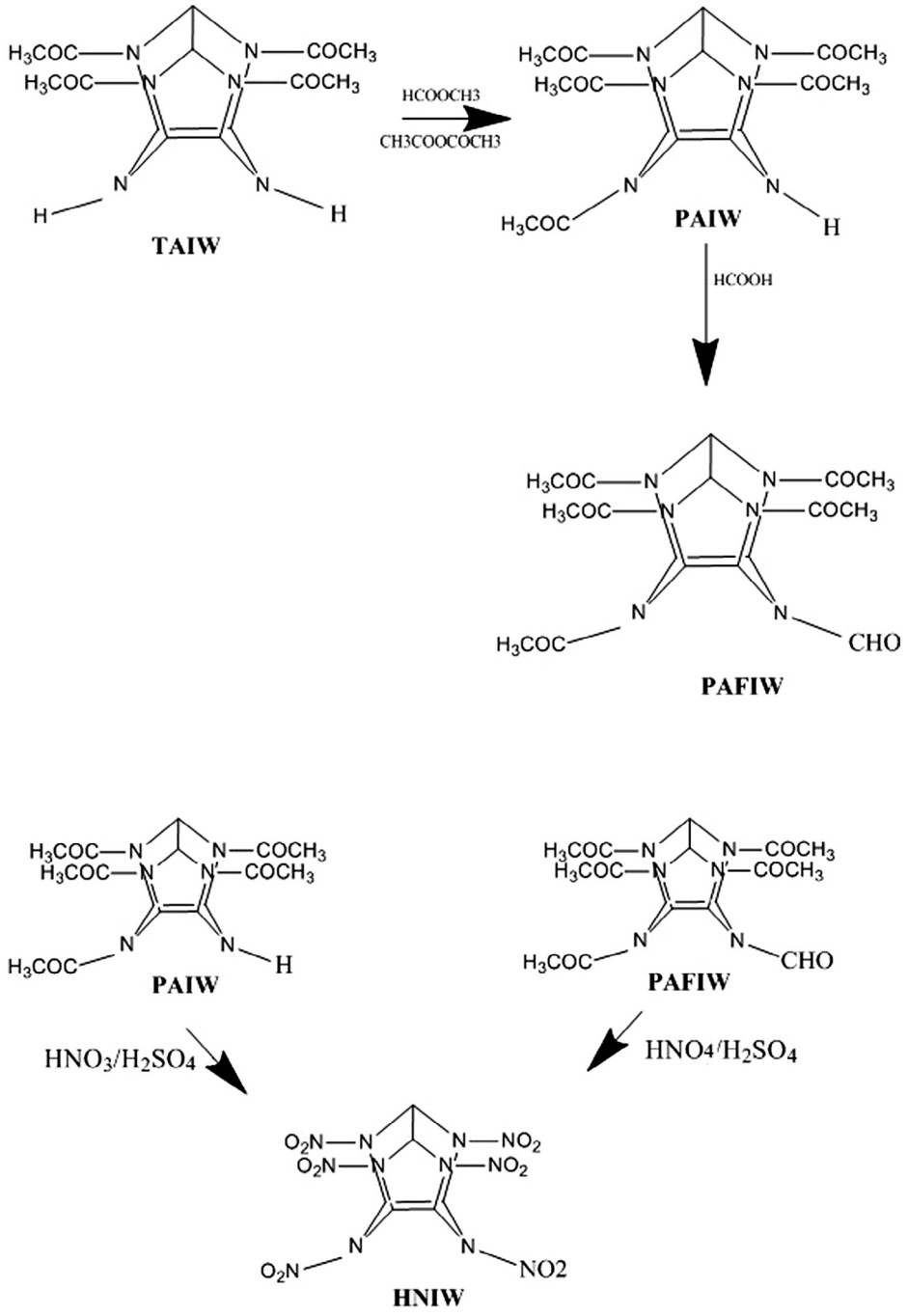

Fig. 11. Synthesis of HNIW through PAIW/PAFIW.

4. Investigation on studies of HNIW and its polymorphs

4.1. Structure

The difference in the orientation of nitro groups with respect to the FMR and SMR of HNIW cage structure is responsible for the occurrence of different polymorphs. The polymorphs of HNIW have different densities and different properties. This particular behavior is due to the difference in crystal lattice packing and number of molecules per unit cell. The increased dihedral angle of FMR leads to the increase in the bond length between the carbon atoms that bound two FMRs together. The increase in the bond length causes the weakening and tension in the bond. This tension is one of the reasons for high energy in the molecule. The negative population between N atom of FMR and N atom of SMR causes the weak repulsion between these atoms, causing the boat shape of SMR to be unstable. If the dihedral angle between N,C,C,N atoms of planar FMR is about 105–115°, the N—NO_2 linked between them is called v-NO_2 (Vertical-NO_2); if it is about 170–180°, it is called h-NO_2 (Horizontal-NO_2) generally. The increase in N—NO_2 bond length in v-NO_2 (1.44 Å) when compared to h-NO_2 (1.40 Å) is observed, which leads to the fragility of v-NO_2 rather than

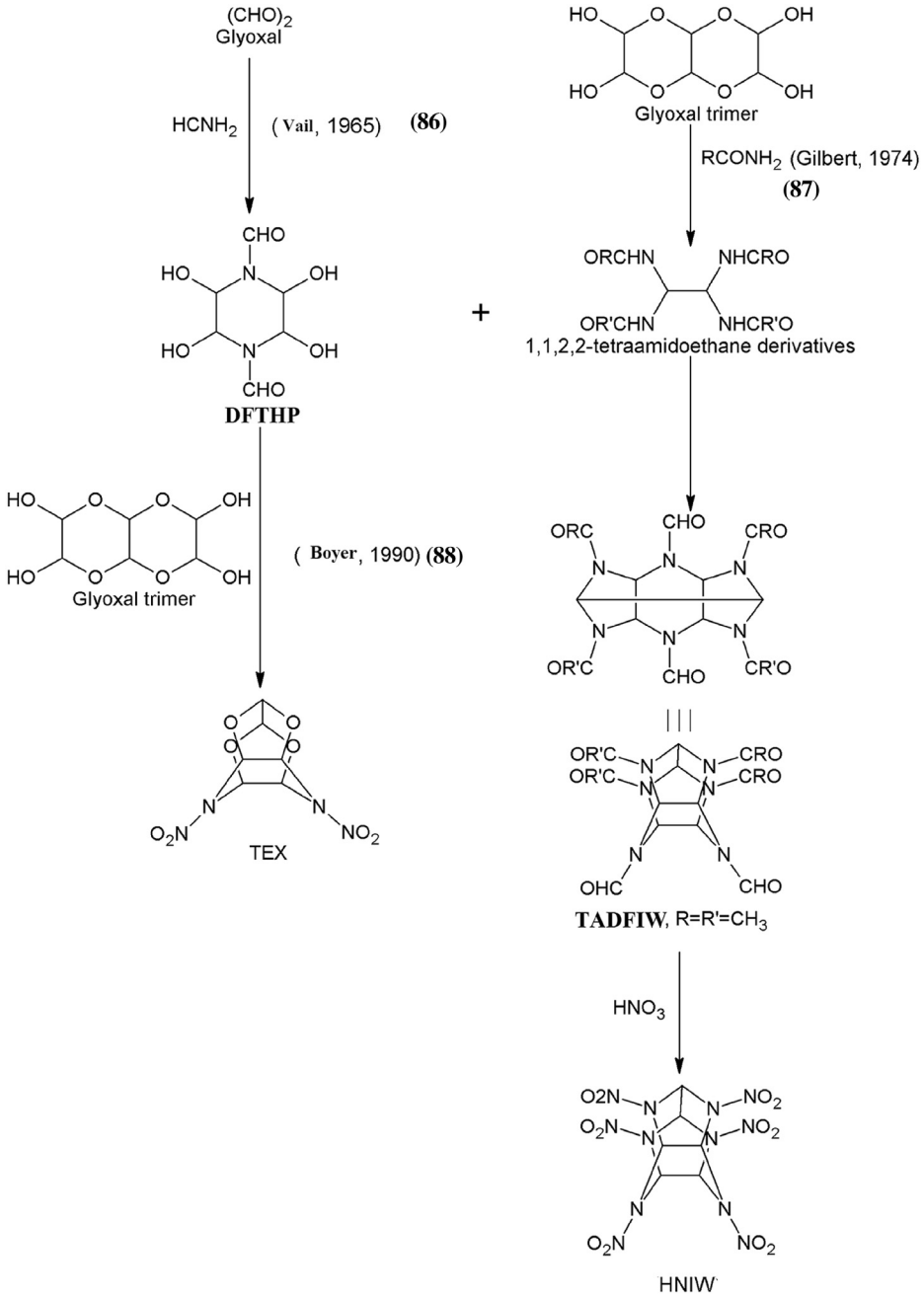

Fig. 12. Benzylamine free synthesis of HNIW.

h-NO_2. This implies more energy to the polymorphs. The polymorph that has more v-NO_2's has more energy in it [17]. The packing parameters are responsible for space groups in the polymorphs. The α- and β-polymorphs of HNIW are orthorhombic Pbca and orthorhombic $Pb2_1a$ respectively, whereas the γ- and ε-polymorphs have same space group (monoclinic $P2_1/c$) [63]. The difference in γ- and ε-polymorphs is observed structurally. The four different HNIW polymorphs are molecular crystals in which dipole–dipole interactions are strong and comparable with van der Waals interactions. Although the energies of van der Waals and dipole–dipole interactions in HNIW polymorph crystals are substantially different, the average deviation of the total energy for the four conformers of HNIW is approximately 0.0011 a.u. This particular behavior restricts the synthesis of a single conformer. However the synthesis of a particular conformer is based on the proper choice of the solvent as per structural characteristics of the conformer. The tension in the cage is explained by the populations between corresponding atoms, which are negative except for the carbon atoms which bind the two FMRs in HNIW. The almost equal population of C—C bond of two FMRs and six bonds of SMR infers the high strength of the bonds. The increased bond length of C—C (binds FMRs) is in the range of 1.59 Å–1.60 Å, whereas the alkane C—C bond length is 1.54 Å. This increase

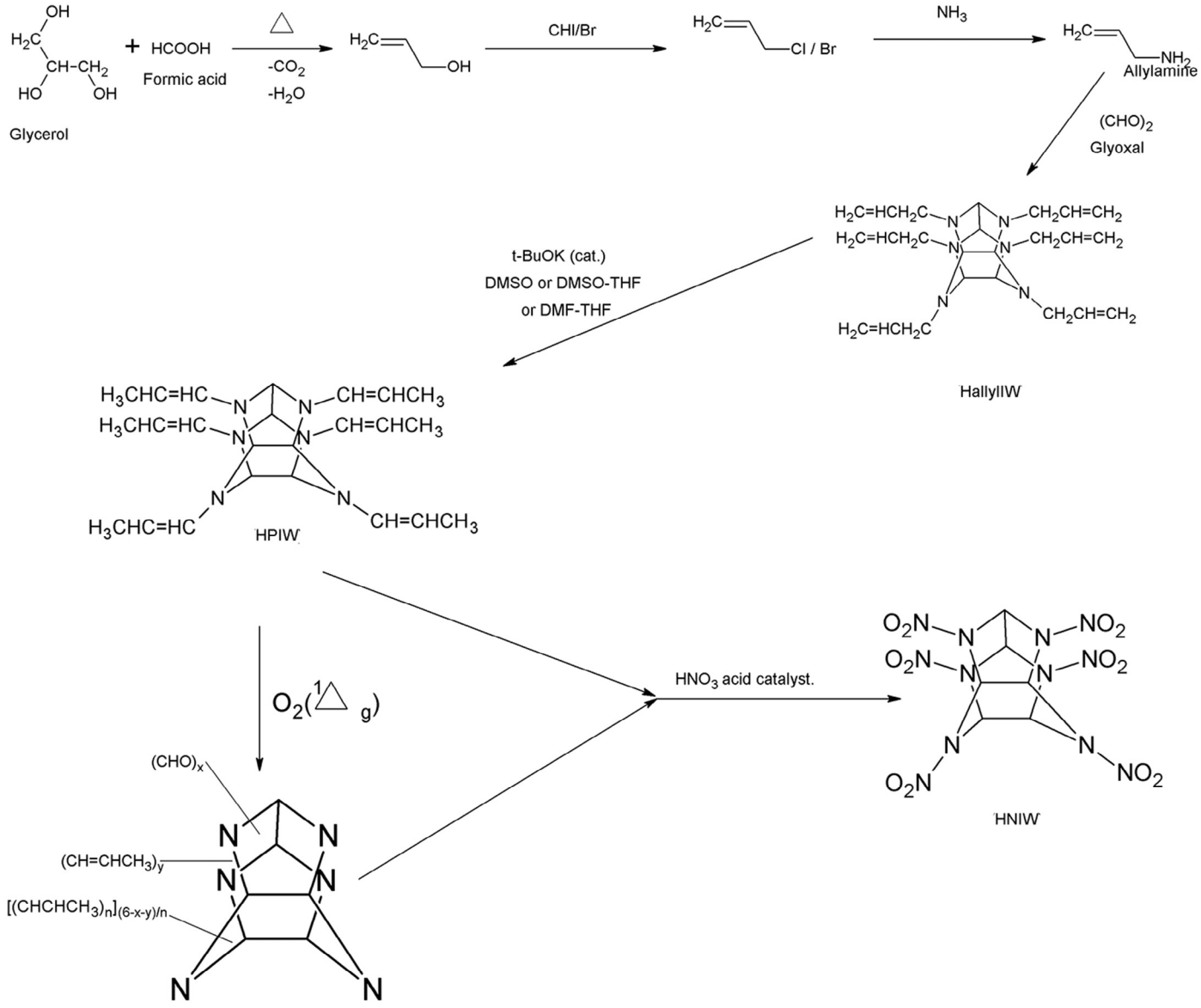

Fig. 13. Benzylamine free synthesis of HNIW through HPIW.

in bond length of HNIW gives tension to the cage. The C—C bond length (binds FMRs) of γ-HNIW is 1.593 Å and is considered to be the shortest among all conformers, which causes the strain in FMR thereby inducing tension in the skeleton. The dihedral angle of SMR taken from D and D′ in HNIW are slightly larger (56.3°) than the dihedral angle of the normal boat shaped hexagon ring (54.0°). This difference in the angle causes the induced tension in SMR [17]. The discussion on energetics of isowurtzitane skeleton is mentioned in the later part of this overview.

4.2. Morphology

Foltz et al. [63] have discussed the morphology of four (α-, β-, γ- and ε-) different forms of HNIW. The authors [63] have identified that the γ-form grows with only needle habitant, whereas the β-form has small prismatic crystals that are solvent dependent. These crystals may possess morphology, viz., needles, prisms or clusters of chunky prisms. Usually a mixture of this is present where the α-form is predominantly prism shaped. Low temperature β→α and β→γ phase transitions are reported. The morphology of the ε-form is mostly irregular shape and at places large crystallites are observed.

4.3. FTIR

Ghosh et al. [61] observed the typical vibration bending modes of —ONO and —NO for different polymorphs of HNIW in the region 738.2–770.0 cm^{-1}. It is observed that α-form shows a strong doublet in the region. The β-form has a weak multiplet peaks in the region 738.2–750.0 cm^{-1} and a strong peak around 765.0 cm^{-1}. The ε-form has quartet in the region 738.2–758.2 cm^{-1}. In the γ-form, the FTIR spectrum is similar to α-form, except that the peak around 750 cm^{-1} is broad along with a very weak splitting in this region. The other peaks in the higher wavelength region are almost similar for all

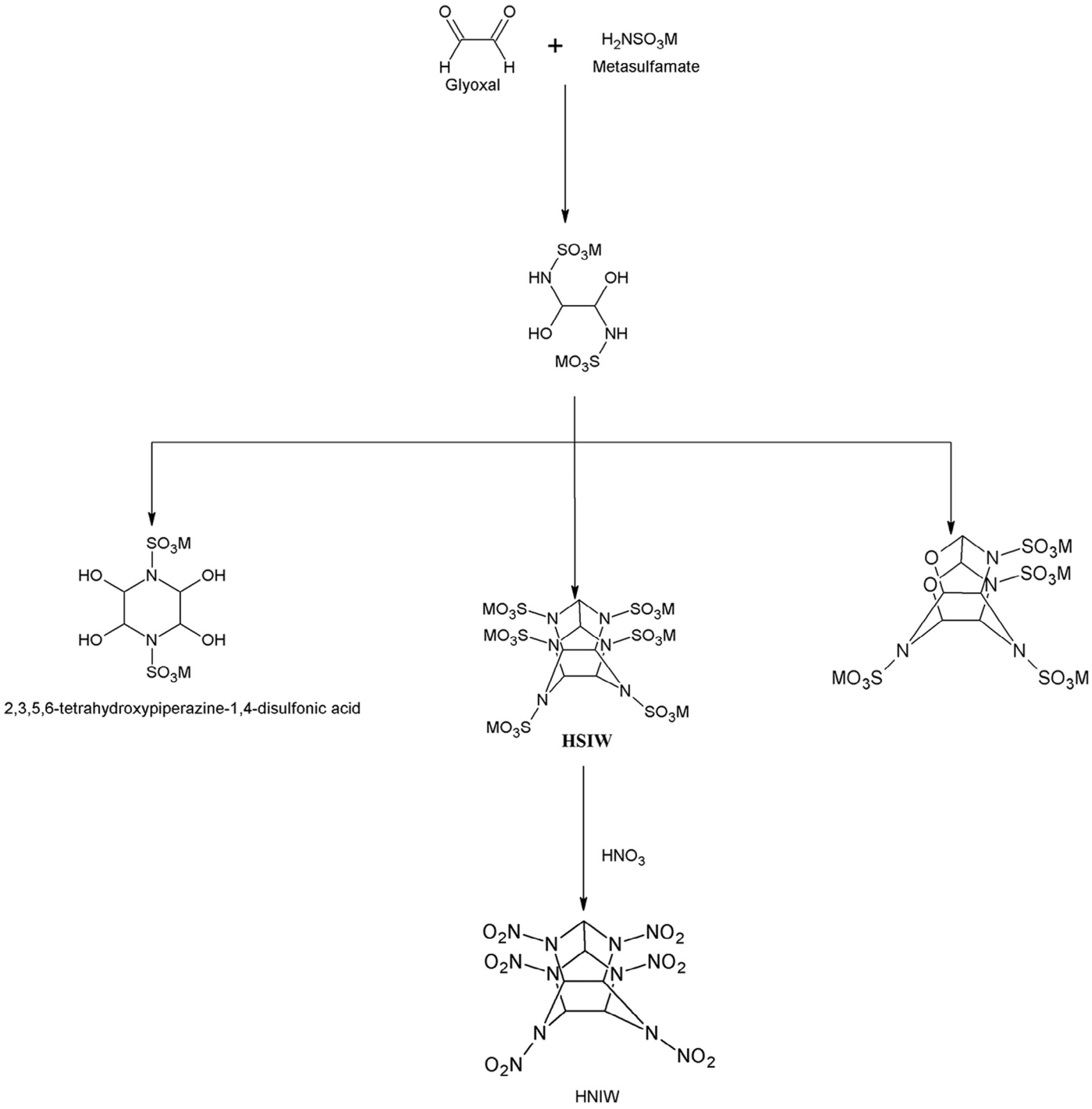

Fig. 14. Synthesis of HNIW from metal sulfamate and glyoxal precursors.

the morphological forms. Hence it may be cautiously stated that the region 738.2–770.0 cm^{-1} may be considered as the fingerprint region in elucidating the polymorphic structure of HNIW. Another interesting feature is observed around 950.0 cm^{-1} for all the polymorphs. The α-form shows a single maximum intensity peak, which is comparable to that of γ-form observed in the same wavelength region. While the β-form shows splitting of the maximum intensity peak in the region of 950.0 cm^{-1}, the ε-form shows a weak splitting at the same wavelength region.

Raman spectral study of Ghosh et al. [61] also collaborates with the FTIR report of Foltz [22]. There appears a typical 280 cm^{-1} peak corresponding to a ring deformation for α-HNIW. The peak shifted to 264 cm^{-1} in ε-HNIW. The authors

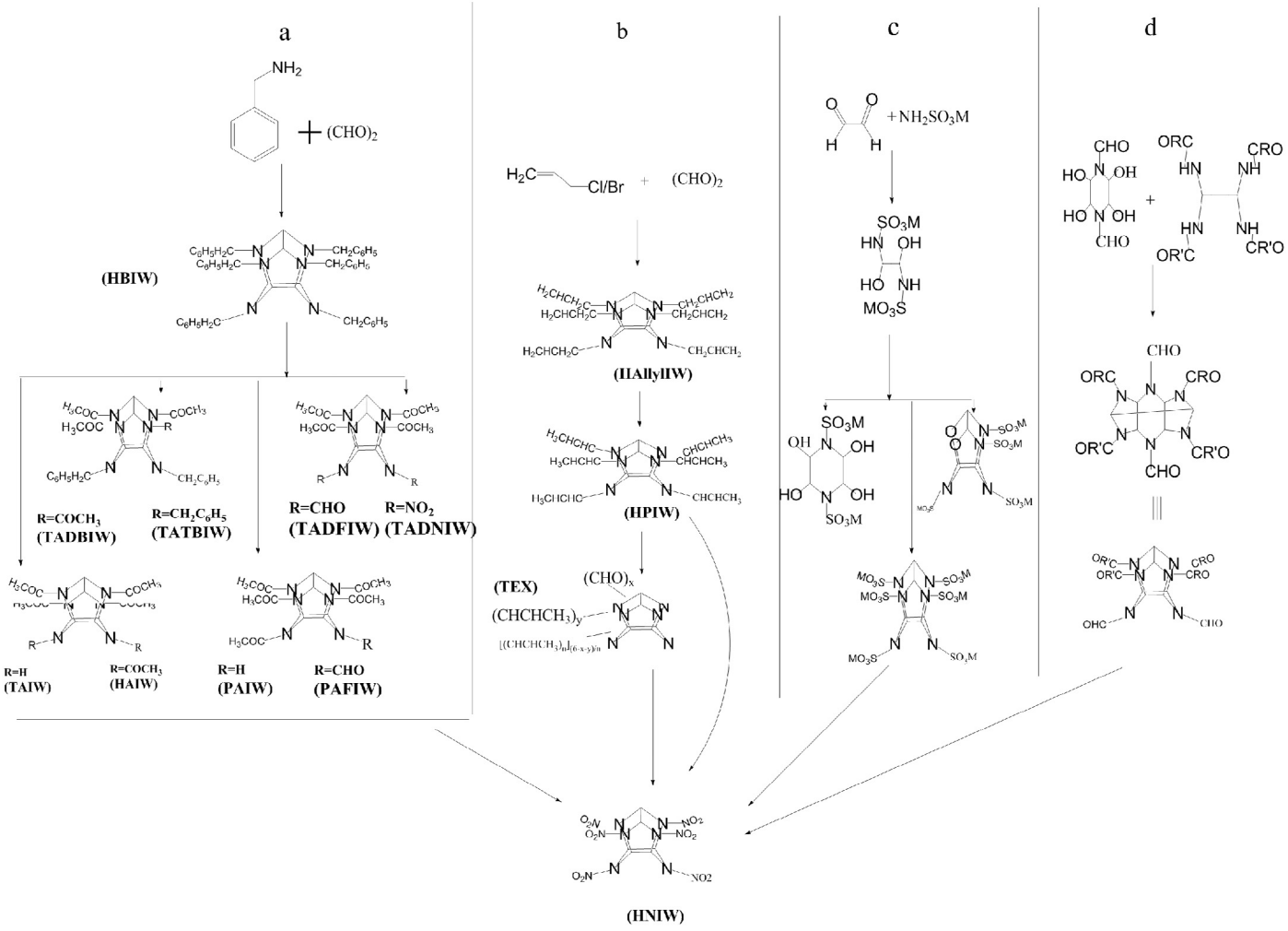

Fig. 15. Organization flow chart.

[61] have reported a distinct peak at 264 cm^{-1} in the range of 260–300 cm^{-1}, which indicates the formation of pure ε-HNIW.

4.4. Thermal studies

The thermal study for the different polymorphs of HNIW is reported by many workers [22,33,63]. It is conclusively understood that the decomposition of the different polymorphs of HNIW undergoes a solid state reaction [33], which is contradictory to other solid HEMs. The α- and the ε-forms are converted to γ-form at around 160 °C, while the β-form is unstable as represented by the P–T phase diagram for the different forms of HNIW [33]. Also the α-form is a hydrated one when the conversion to γ-form takes place. Hence the thermal study of HNIW is understood by the study of the γ-form. The conversion of α/ε forms to γ-form is collaborated by Foltz [22] through an FTIR spectral study, which collaborates the observations made in thermal study. The phase transformation at high pressures (up to 5 MPa) is unaltered according to Gump and Peiris [64]. The authors [64] have identified the γ-phase at 120–125 °C which is stable up to 150 °C at both ambient temperature and at 75 °C. The synchronous angle dispersive X-ray diffraction study was used to identify the phases at different stages of the study. The regular ε→γ phase transition for ε-HNIW occurred at 125 °C, whereas the ε→γ phase transition was identified at 56.5 ± 1.5 °C for ε-HNIW incorporated into polar plasticizers and polar polymeric binders (polyGLYN, polyNIMMO, etc.) by Torry and Cunliffe [65]. Tian et al. [66] have observed the physical changes in HNIW sample when the sample was subjected to temperature effect. The HNIW sample showed volume expansion and after phase transition to γ-form (around 160 °C), the sample acquired very rough surface with numerous dimple depressions. The large number of voids was produced on the surface and the bulk which collaborated by the author [66] from their AFM and SAXS studies. Zhang et al. [67] have carried out an interesting study on the role of different additives on the phase transformation of ε→γ, and concluded their observations based on the collaborative results obtained from thermal analysis data with powder X-ray diffraction patterns. The authors [67] have reported a modest decrease in the phase transformation temperature of ε→γ form when polar solvents, viz., DOA, were employed. The solvent has interfacial bonding with the outer crystal faces of the ε-HNIW, making the crystal to dissolve and thus aid in ε→γ transformation. However, when a non-polar solvent like liquid paraffin is added, there appeared to

have no change in phase transformation temperature. The authors opined that the process of phase transformation from ε→γ is dominated both kinetically and thermodynamically. They also observed that the additives, viz., HTPB, AP, and Al, have no effect on the phase transformation temperature; however, when HTPB and TDI binders having poor thermal conductivity are coated onto the ε-HNIW, heat transfer to the inner crystal was blocked thereby inhibiting the polymorphic transformation.

4.5. Chemical decomposition

Yang and Xiao [68] have reported the studies on the chemical decomposition of HNIW, employing the following methodology: electron impact (EI) with metastable mass analyzed ion kinetic energy (MIKE) and chemical ionization (CI) with collision-induced dissociation (CID).

Decomposition of HNIW is initiated with the breakage of N—NO_2 (homolytic cleavage) at FMR, which triggers the molecular decomposition. This is elucidated from the cleavage reaction of $[m/z = 392]^+ \rightarrow [m/z = 316]^+$ in EI [69]. It is further confirmed by photodecomposition of HNIW by ultraviolet light [70], least endothermic heat loss occurring through the elimination of NO_2 from FMR [71], thermal decomposition of ^{15}N-HNIW [72] selective protonation of FMR N—NO_2 group. This behavior along with increased bond length of C—C (binds FMRs) infers that, on the basis of thermal decomposition, N—N bond is the weakest followed by C—N bond, which is then followed by C—C bond.

The authors have reported that the removal of 5 of 6 nitro groups from HNIW is easier, but the last nitro group is intact and the residue molecule formed is stable. The CID mass spectrum of HNIW revealed that the parent fragment at m/z 209 is 100% abundant, whereas the parent fragments at m/z 347, 301 and 255 are relatively abundant. This infers that the loss of 2–5 nitro groups from HNIW during decomposition is easier. The decomposition of parent fragments m/z 347 revealed that the daughter fragment m/z 162 is least abundant. This indicates that loss of the last nitro group from HNIW is difficult, which is also confirmed by the empirical formula of the residue ($C_4H_4N_4O_2$) [73].

Both the EI spectrum and MIKE spectrum showed that the decomposition of m/z 346 parent fragment infers the loss of NO_2 or NO is easier under EI, and the daughter ions $[HNIW + H\text{-}nNO_2]^+$ ($2 < n \leq 5$) are common for the most of the parent fragments with higher molecular weight. Naik et al. [74] have further reported that the ions at m/z 163 or less removes HCN molecule, whereas the ions at m/z 200 to m/z 300 may form NO_2, NO and HCN. The removal of pyrazine ion is also reported at m/z 108.

The pyrolysis gas chromatography coupled with mass spectrometry (EI) performed by Naik et al. [74] has revealed fragments in the range m/z 80–125 correspond to substituted pyrazine derivatives. The presence of NO, N_2 and N_2O is confirmed by m/z 30, 28 and 44 respectively. HCN formed during pyrolytic decomposition of HNIW will further decompose to form cyanogen gas (C_2N_2). This is observed at m/z 52. The N—N bond rupture responsible for the decomposition of both FMR and SMR of HNIW leads to the formation of NO, NO_2 and HONO. Some of the substituted pyrazine derivatives further decompose to lower molecular fragments and forms H_2O, HCN, CO, HNCO, CO_2 and C_2N_2. The authors have proposed a pyrolytic decomposition mechanism in their literature.

From these studies it is concluded that homolysis of N—NO_2 bond and break up of C—C (binds FMRs) are considered to be an important initial process in the thermal decomposition of HNIW.

4.6. Energetics

The values of heat of combustion and formation deserve a mention in understanding the conventional ring strain energy (CRSE) of the compounds. The CRSE for isowurtzitane is 108.0 kJ/mol [8] and is similar to that of cyclopropane and cyclobutane. This value of CRSE is far less than the recently reported HEMs like octanitrocubanes (ONC), which has a value of 685.8 kJ/mol. An important observation was made by Turker [16] in his work on the stability of cage structure of HNIW, and its decomposition when bombarded by α-particle. Employing the DFT, Turker found that the removal of single NO_2 group from the FMR or the SMR of CL-20 causes cage destruction in dication form. This study is important as it involves tagging of neutron with classical explosives for detection [75]. The isowurtzitane skeleton is stable even under the influence of electrostatic forces; however, a removal of NO_2 group makes the cage structure of CL-20 unstable. Hence, the higher heat of formation is associated not only with the formation of cage structure but essentially with the presence of the NO_2 groups.

4.7. Solubility

The greater is the solubility, the greater is the change in the particle size distribution with time. In addition, formulations based on polymorphic HEMs can witness phase conversion to metastable polymorphs when stored at a temperature above that of conversion. Temperature cycling exacerbates recrystallization of the HEMs into metastable polymorphs. This conversion to high temperature stable, lower density polymorphs is variably accompanied by crystal dilatation. As a result, localized phase conversion of the crystalline HEMs to a metastable phase will cause undesirable volume expansion and stress-cracking [22].

4.8. Impact sensitivity and its modification

Impact sensitivity is one of the shock sensitivities where the explosive nature (insensitivity in munitions) is measured when it is stricken with a known weight and from a known height. The impact sensitivity is measured in impact energy (h_{dr}) in "J" or drop height in which 50% of the sample exploded ($h_{50\%}$) in "cm". HNIW is one of the best and efficient nitramine explosives, but its applicability is restricted for its sensitiveness (4.1 J for ε-HNIW). There happened to be a vast research on decreasing the sensitivity toward impact for HNIW. The successful efforts put forth so far are consolidated here. The impact sensitivity of HNIW depends on various factors including morphology, steric effect of reaction center, intermolecular

interactions and so on and so forth. The modifications in these factors have been attributed to the decrease in the impact sensitiveness of HNIW. The effect of modifications and their impact over impact sensitivity are listed below.

4.8.1. Morphology

During the solvent–antisolvent crystallization process, removal of impurities and residual solvent from crystals aided in decreasing the impact sensitivity along with the elimination of cracks, smoothening and reduced particle sizes [76]. The authors [76] in their report have observed that recrystallization of α-HNIW to ε-HNIW by adding n-heptane as anti-solvent to the ethyl acetate solution gives lower porosity, particle size of 51.5 μm and 50% probability of initiation with impact energy (E_{dr}) of 1.86 J, while the inverse crystallization using ethyl acetate solvent with silica gel (drying agent) and n-heptane anti-solvent gives lower crystal size (31.8 μm) and 2.34 J of increased impact energy. The crystallizations by the assistance of ultrasound gives regular crystal shapes with some cracks, smaller particle size (14.2 μm), narrow particle size distribution and a higher impact energy of 4.12 J. The crystallization of HNIW by adding admixtures removes impurities and residual solvent from the crystal, thereby forming regular uniform morphology, small particles (9.1 μm) without sharp edges possessing much higher impact energy of 10.83 J.

4.8.2. NMR studies

The ^{13}C NMR chemical shifts for HNIW showed that the impact sensitivity depends on the electronic configuration at the reaction center of the molecule and intermolecular interactions in the crystal [77]. However, ^{15}N NMR of HNIW discussed below reported that chemical shift values inferred that impact sensitivity depends on both electronic configuration and steric effect along with the intermolecular interactions [78]. The study of ^{15}N NMR of the N_{aza} also named as "chemical hot spots" and N_{nitro} gives information on the electronic configuration and steric condition of the reaction center on the molecule. The chemical shift observed in such molecules is influenced by nitrogen hybridization, size of the crystal, conformation and the extent of lone pair on N_{aza} involved in π-bonding with the nitro group. Jungova et al. [78] have concluded that the HNIW molecule possesses two types of chemical shifts "δ". In case of FMR N_{nitro} the δ is −40.30 ppm, and that for N_{aza} it is −199.00 ppm, whereas in the case of SMR, the N_{nitro} δ is −43.40 ppm, and that for N_{aza} is 179.50 ppm. The difference observed in both the N_{aza} and N_{nito} of FMR and SMR indicates that the chemical hot spots are different in both, i.e., SMR and FMR. Jungova et al. [78] reported a new product named as "Reduced Sensitivity-ε-HNIW", with an impact sensitivity of 8–12.6 J, commercially called as "RS-ε-HNIW" synthesized through crystal engineering, which is discussed later in this overview. The authors [78] also discussed the impact factor (based on drop energy) with respect to ^{15}N NMR studies, and observed that the normal ε-HNIW falls apart from the specified correlated line, while the RS ε-HNIW falls on this correlated line. This indicates the decrease in impact sensitivity of RS ε-HNIW when compared with normal ε-HNIW.

4.8.3. Crystal engineering effect

The dependence of impact sensitivity of HNIW on the crystal morphology and particle size distribution is of greater importance. These physical parameters can be modified by adding additives, promoters or by physical means, and the process is called crystal engineering. The effects of some crystal engineering strategies of HNIW on impact sensitivity are listed below.

4.8.3.1. Additive. Recrystallization of γ-HNIW to obtain ε-HNIW through the addition of three different additives, viz., ethylene glycol, triacetin, andaminoacetic acid at a dosage of 0.3 weight%, showed different morphology. Chen et al. [79] have employed ethylacetate as solvent, and trichloromethane as antisolvent. This study showed a reduction of crystal face area ratio in the order aminoacetic acid > triacetin > ethylene glycol. The crystal morphology changed from bipyramidal for pure ε-HNIW to cuboid, cube and spherical morphologies when ethylene glycol, triacetin and aminoacetic acid are respectively added. The morphology change described above is due to the crystal face area ratio {110}:{200}. The crystal face area ratio of ε-HNIW is in the order of pure > ethylene glycol > triacetin > aminoacetic acid. The impact sensitivity values ($h_{50\%}$) for pure HNIW and additive added ones (ethylene glycol, tiacetin and aminoacetic acid) are 25.5, 36.4, 41.8, and 52.6 cm respectively. It is observed that the change in shape of the crystal from dipyramidal to spherical decreases the impact sensitivity, thereby confirming that aminoacetic acid additive gives reduced impact sensitivity [79].

4.8.3.2. Ultrasound assisted precipitation. Sonication is a process of achieving fine particles with narrow size distribution, from coarse particles. An increase in impact sensitivity from 28 cm to 44 cm is achieved for samples without and with sonication respectively [80]. Sonication also reduces the time of addition of antisolvent (e.g. heptane fraction to ethyl solution) during the process of recrystallization.

4.8.3.3. Promoters. It is understood that during crystal engineering of HNIW, generation of cubic or spherical shaped crystals will reduce the impact sensitivity of HNIW [79] when compared with general RDX and HMX.

With the addition of compound promoters possessing nonbonding interactions with HNIW (viz., amino acids like glycine, alanine and esters of them, polyols like poly(vinyl alcohol), glycerol, pentaerythritol and others, organic acids like butane carboxylic, maleic, malonic, adipic acids, etc., and their esters) into the saturated solution, before the addition of a suitable antisolvent, and by using a suitable method for HNIW precipitation from the resulting solution gave ε-HNIW crystals (called as RS-ε-HNIW) with rounded edges, minimal defects and less impurities. This RS-ε-HNIW of 98% purity possesses impact sensitivity ranging from 5.6 J to 10.2 J [81]. In another method, Doo [82] has used pyridine as a promoter under different experimental conditions and obtained the impact sensitivities in the range of 8.1–12.7 J. Recently Zeman et al. [83,84] have reported a reduced impact sensitivity of 10.8 J with 99.8%

of purity for HNIW by using phosphorous pentoxide (P_2O_5) as a promoter.

4.9. Binder formulation

HNIW composite energetic material with binders like GAP/THMNM/NC/HDI to form monolithic gels was synthesized (sol-gel method) and was evaluated by Li and Brill [85]. The increased loading capacity (90%) of HNIW was reported. The polymorphic transition from ε- to α-HNIW was reported during gelation with different binders. The reduced thermal stability of composites reported by the authors [85] is due to the hydrogen bonding and dipolar interactions between N—NO_2 of HNIW and polar groups of polymer gels. The lowered decomposition temperature (40–60 °C) and reduced impact sensitivity (15–33 H_{50}/inch) are the benefits reported by this composite energetic material formation.

4.10. Derivatives

A theoretical investigation on the derivatives of HNIW (4-trinitroethyl-2,6,8,10,12-pentanitrohexaazaisowurtzitane) is predicted by Li et al. [34]. These authors, on the basis of density function theory, predicted the packing density, velocity of detonation and the infrared spectrum of the derivative molecule. The values are higher than that of the pure HNIW and other analogs, indicating that the derivative will be better HEM with an added thermal stability.

4.11. Cocrystals

Currently, more and more energetic cocrystals are being found, opening a road to HEMs with tuned properties. The energetic cocrystals are crystals containing two or more neutral molecular components in which at least one is energetic. These molecules rely on noncovalent interactions to form a regular arrangement in crystal lattice. It is termed as "energetic cocrystallization engineering" that alters the stacking mode of existing energetic molecules and related properties like power (energy) and safety (sensitivity). This strategy is becoming a unique approach to new HEMs and LSHEMs. Recent works on synthesis of new materials by fusing a sensitive and a less sensitive material to achieve better packing density and higher velocity of detonation through the process of cocrystallization are reported. The above mentioned characteristics are achieved by forming cocrystals of HNIW/BTF, HNIW/HMX, HNIW/TNT, etc. The intermolecular interactions and hydrogen bonds formed between the components of cocrystals aid in achieving better characteristics than the constituent HEMs [35,36a,b,37]. Yang et al. [35] provides the evaluations of power (energy) and safety of a good number of observed binary energetic cocrystals, by studying their density (ρ), oxygen balances (OB), explosive properties and crystal morphologies with the aid of theoretical calculations. The authors [35] showed that cocrystallization increases the safety (insensitivity) with a possible decease in power. The synthesized cocrystal density, OB and morphology are understood to change from their respective constituents, thus becoming a unique approach to new HEMs and LSHEMs.

This overview envisages the importance of cocrystallization in achieving high packing density and lower impact sensitivity when compared with constituent HEMs. The ε-HNIW/BTF cocrystal (nitramine-furazan cocrystal) has intermolecular interactions and hydrogen bonds between ε-HNIW and BTF. The intermolecular interactions were reported between electron rich nitrogen atoms of HNIW and electron poor ring of BTF and the hydrogen bond was reported between H(C) of ε-HNIW and nitrogen atom of BTF [35]. Zhang et al. [36a] have studied the HNIW/TNT or HNIW/HMX cocrystals are reported to have hydrogen bonding between H(C) of HNIW and oxygen of TNT or HMX [36a]. The authors have reported that the $O\cdots H$, $O\cdots O$, $N\cdots O$ interactions dominated the intermolecular interactions in the cocrystals based on Hirshfeld surfaces, radial distribution function, interaction energy and electronic structure of pure co-formers and cocrystals [36a].

Wei et al. [36b] have studied the changes in the three thermodynamic parameters (changes in internal energy (ΔE), enthalpy (ΔH), and Gibbs free energy (ΔG)), along with the difference in solubility parameters (Δδ), to quantitatively evaluate the thermodynamics of EECC formation. The authors, on the basis of the calculated results of ΔE, concluded that EECC formation is not always energetically favored.

5. Conclusion

In spite of various routes obtained for HNIW synthesis, the present cost of the substance is far high. Modified procedures are required to accomplish cost effectiveness and mass manufacture. Deep view on compatibility as well as consistency based aspects for the synthesis of HNIW is required. The low cost and the advantages of Procedures 2 and 3 in this overview make them the best methods among the remaining existing procedures. The scope of reducing both time and cost of production for HNIW came on to the reaction desks of scientist with the use of glyoxal and metal sulfamate as precursors. The two-step method for synthesis of HNIW is attracting the attention of the entire high energy materials research world. The understanding of probable reactants' ratio of the non-hazardous precursors and reaction conditions is needed to synthesize HNIW effectively in the large scale. The proposed synthesis procedure [30] may effectively overcome the barrier of large scale synthesis economically. Decreased impact sensitivity of HNIW allows its applicability in various fields. Note on parameters to decrease the impact sensitivity of HNIW may help the manufacturers to take due care at the time of synthesis. It is now being understood that cocrystals with the required characteristics possibly play an important role in future weaponry, propellant and HEMs.

Acknowledgment

The authors J.V.V and V.K.J are thankful to Dr. A.N. Gupta, CMD, Premier Explosive Limited, India, for the kind support and financial assistance under the sponsored project "Novel materials for high energy reactions" (H/A: 4254) to Gulbarga University, Kalaburagi, India. The authors A.V.R and N.V.S.R are thankful to Dr. A.N. Gupta for the helpful discussion on the topic.

References

[1] Nielsen AT. Caged polynitramine compound. U.S.Patent 5693794; 1997.

[2] Panikov NS, Sizova MV, Ros D, Christodoulatos C, Balas W, Nicolich S. Biodegradation kinetics of the nitramine explosive HNIW in soil and microbial cultures. Biodegradation 2007;18:317–32.

[3] Pavlov J, Christodoulatos C, Sidhoum M. Hydrolysis of hexanitrohexaazaisowurtzitane (HNIW). J Energetic Mater 2007;25: 1–18.

[4] Heilmann HM, Wiessmann U, Stenstrom MK. Kinetics of the alkaline hydrolysis of high explosives RDX and HMX in aqueous solution and adsorbed to activated carbon. Environ Sci Technol 1996;30:1485–92.

[5] Aerotech news and overview, development on C. J Aeros. Def: Indust. News; 2000.

[6] Golfier M, Graindorge H, Longevialle Y, Mace H. New energetic materials and their applications in energetic materials. In: Proceedings of the 29th international annual conference of ICT, Karlsruhe, Federal Republic of German; 1998. p. 03/1–18.

[7] Braithwaite PC, Hatch RL, Lee K, Wardle RB. Development of high performance HNIW explosive formulations. In: 29th International Annual Conference of ICT, Karlsruhe, Federal Republic of Germany; 1998. p. 04/1–7.

[8] Bumpus JA. A theoretical investigation of the ring strain energy, destabilization energy, and heat of formation of HNIW. Adv Phys Chem 2012;doi:10.1155/2012/175146.

[9] Nair UR, Sivabalan R, Gore GM, Geetha M, Asthana SN, Singh H. Hexanitrohexaazaisowurtzitane (HNIW) and HNIW-based formulations. Combust Explos Shock Waves 2005;41(2):121–32.

[10] Bircher SR, Mader P, Mathieu J. Properties of HNIW based high explosives. In: 29th InternationalAnnual Conference of ICT, Karlsruhe, Federal Republic of Germany; 1998. p. 94/1–14.

[11] Bellamy AJ. Reductive debenzylation of hexabenzylhexaazaisowurtzitane. Tetrahedron 1995;51(16):4711–22.

[12] Krause HH. Teipel U, editor. New energetic materials. Weinheim: Wiley-VCH Verlag GmbH & Co. KGaA; 2005.

[13] Mandal AK, Pant CS, Kasar SM, Soman T. Process optimization for synthesis of HNIW. J Energ Mater 2009;27:231–46.

[14] Borman S. Advanced energetic materials emerge for military and space applications. Chem Eng News 1994;72(3):18–22.

[15] Bottaro J. Recent advances in explosives and solid propellants. Chem Ind 1996;10:249–53.

[16] Turker L. Instability of CL-20 exposed to the effect of α-particle. Ind J Chem 2015;54A:858–66.

[17] Zhou G, Wang J, He WD, Wong NB, Tian A, Li WK. Theoretical investigation of four conformations of HNIW by B3LYP method. J Mol Struct (Theochem) 2002;589590:273–80.

[18] Simpson RL, Urtiew PA, Ornellas DL, Moody GL, Scribner KJ, Hoffman DM. CL-20 performance exceeds that of HMX and its sensitivity is moderate. Propellants Explos Pyrotech 1997;22(5):249–55.

[19] Talawar MB, Sivabalan R, Anniyappan M, Gore GM, Asthana SN, Gandhe BR. Emerging trends in advanced high energy materials. Combust Explos Shock Waves 2007;43(1):62–72.

[20] Murray JS, Concha MC, Politzer P. Links between surface electrostatic potentials of energetic molecules, impact sensitivities and C-NO_2/N-NO_2 bond dissociation energies. Mol Phys 2009;107(1):89–97.

[21] Yu L, Ren H, Guo XY, Jiang XB, Jiao QJ. A novel-HNIW-based insensitive high explosive incorporated with reduced graphene oxide. J Therm Anal Calorim 2014;117(3):1187–99.

[22] Foltz MF. Thermal stability of ε-hexanitrohexaazaisowutzitane in estane formulation. Propell Explos Pyrot 1994;19:63–9.

[23] Nielsen AT. The synthesis of HNIW (HNIW, 6) from its precursor, 4,10-dibenzyl-2,6,8,12,-tetra acetyl-2,4,6,8,10,12-hexaazaisowurtzitane. US Patent Office Application Case No. 70631, US Dept of Navy; 1987.

[24] Gore GM. Synthesis and scale-up of hexanitrohexaazaisowurtzitane (HNIW). Pune, India: Energetic Materials Division, High Energy Materials Research Laboratory; 2006 (unpublished work).

[25] Latypov NV, Wellmar U, Goede P. Synthesis and scale-up of 2,4,6,8,10,12-hexanitro-2,4,6,8,10,12-hexaazaisowurtzitane from 2,6,8,12-tetraacetyl-4,10-dibenzyl-2,4,6,8,10,12-hexaazaisowurtzitane. Org Process Res Dev 2000;4:156–8.

[26] Guan XP, Yan H, Sun JG, Yu YZ. Novel carbon-carbon bond oxidative cleavage of hexabenzylhexaazaisowurtzitane by n-BuONO and $(NH_4)_2Ce(NO_3)_6$. Molecules 1999;4(3):69–72.

[27] Ghosh M, Venkatesan V, Sikder N, Sikder AK. Quantitative analysis of α-HNIW using dispersive Raman spectroscopy. Cent Eur J Energ Mater 2013;10(3):419–38.

[28] Jiang X, Guo X, Ren H, Jioa Q. Preparation and characterization of desensitized ε-HNIW in solvent-antisolvent recrystallizations. Cent Eur J Energ Mater 2012;9(3):219–36.

[29] Gore GM, Sivabalan R, Nair UR, Saikia A, Venugopalan S, Gandhe BR. Synthesis of CL-20: by oxidative debenzylation with cerium (IV) ammonium nitrate (CAN). Indian J Chem 2007;46(B):505–8.

[30] Chapman RD, Richard AH, Thomas JG, David AN. SERDP SEED Project WP-1518, Benzylamine-free, heavy-metal-free synthesis of HNIW. Naval Air Warfare Center Weapons Division China Lake, and Naval Air Systems Command Principal Investigator: Chemistry Branch. (Code 498200D) Research Division Research & Engineering Sciences Department Naval Air Warfare Center Weapons Division 1900 N. Knox Rd. Stop 6303 China Lake, CA 93555-6106, 28 December 2006; 2.

[31] Chapman RD, Hollins RA. Processes for preparing certain hexaazaisowurtzitanes and their use in preparing hexanitrohexaazaisowurtzitane. US Patent 7,875,714 B1, USA; 2011.

[32] Agarwal JP, Hodgson RD. Organic chemistry of explosives. Chichester: Wiley and Sons Publications; 2007.

[33] Nedelko VV, Chukanov NV, Raevskii AV, Korsounskii BL, Larikova TS, Kolesova OI, et al. Comparative investigation of thermal decomposition of various modifications of hexanitrohexaazaisowurtzitane (CL-20). Propell Explos Pyrot 2000;25(5):255–9.

[34] Li XH, Cui HL, Li LB, Zhang XZ. Theoretical investigation on crystal structure, detonation performance and thermal stability of a high density cage hexanitrohexaazaisowurtzitane derivative. J Chem Sci 2013;125(4):919–25.

[35] Yang Z, Li H, Zhou X, Zuang C, Huang H, Li J, et al. Characterization and properties of novel energetic-energetic cocrystal explosive composed HNIW and BTF. Cryst Growth Des 2012;12(11):5155–8.

[36] (a) Zhang C, Xue X, Cao Y, Zhou J, Zhang A, Li H, et al. Towards low-sensitive and high energetic cocrystal II: structural electronic and energetic features of CL-20 polymorphs and the observed CL-20 based energetic- energetic cocrystal. Cryst Eng Comm 2014;16:5905–5916; (b) Wei X, Zhang A, Ma Y, Xue X, Zhou J, Zhu Y, et al. Towards low-sensitive and high-energetic cocrystal III: thermodynamics of energetic-energetic cocrystal formation. Cryst Eng Comm 2015;17: 9037–47

[37] Wei X, Ma Y, Long X, Zhang C. A Strategy developed from the observed energetic-energetic cocrystals of BTF: cocrystallizing and stabilizing energetic hydrogen-free molecules with hydrogenous energetic conformer molecules. Cryst Eng Comm 2015;17:7150–9.

[38] Sysolyatin SV, Lobanova AA, Chernikova YT, Sakovich GV. Methods of synthesis and properties of hexanitrohexaazaisowurtzitane. Russ Chem Rev 2005;74(8):757–64.

[39] Sysolyatin SV, Sakovich GV, Surmachev VN. Methods for the synthesis of polycyclic nitramines. Russ Chem Rev 2007;76(7):673–80.

[40] Sysolyatin SV, Lobanova AA, Chernikova YT. Method for obtaining the 2,4,6,8,10,12-hexa-nitro-2,4,6,8,10,12-hexa-azo-tetracyclo(5,5,0,$0^{3,11}$,$0^{5,9}$) dodecanes. Russian Patent RU 2,199,540; 2003.

[41] Lowenheim FA, Moran MK. Benzyl chloride (alpha-clorotoulene). In: Faith, Keyes and Clark's Industrial Chemicals. 4th ed. New York: John Wiley & Sons; 1975. p. 145–8.

[42] Nielsen AT, Nissan RA, Vanderah DJ, Coon CL, Gilardi RD, George CF, et al. Polyazapolycyclics by condensation of aldehydes with amines 2. Formation of 2,4,6,8,10,12-hexabenzyl-2,4,6,8,10,12-hexaaza-tetracyclo (5.5.0.$0^{5,9}$.$0^{3,11}$)-dodecanes from glyoxal and benzylamines. J Org Chem 1990;55(5):1459.

[43] Yuxiang O, Huiping J, Yongjiang X, Boren C, Guangyu F, Lihua L, et al. Synthesis and crystal structure of β-hexanitro hexaazaiso wurtzitane. Sci China Ser B: Chem 1999;42(2):217–24.
[44] Bescond P, Graindorge H, Mace H. Process for producing the epsilon form of hexanitrohexaazaisowurtzitane. US Patent No. 5,973,149; 1999.
[45] Han WR, Ou YX, Liu JQ, Wang JL. Synthesis and crystal structure of triacetyltribenzyl-hexaazaisowurtzitane (TATBIW·0.5 H_2O). Chin Chem Lett 2004;15(10):1153–6.
[46] Li LJ, Chen SS, Jin SH, Chen HX, Wang AY. Synthesis and reactivity of triacetyltriformylhexaazaisowurtzitane. Trans Beijing Inst Technol 2007;1:73–6.
[47] Nielsen AT. Synthesis of polynitropolyaza caged nitramines. Chemical Propulsion Information Agency (CPIA); 1987. p. 473.
[48] Wardle RB, Edwards WW. Hydrogenolysis of 2,4,6,8,10,12-hexabenzyl-2,4,6,8,l0,l2-hexaazatetracyclo(550.$0^{5,9}$.$0^{3,11}$) dodecane. US Patent No. 5,739,325; 1998.
[49] Wardle RB, Edwards WW. Hydrogenolysis of 2,4,6,8,10,12-hexabenzyl-2,4,6,8,10,12-hexaazatetracyclo[5.5.0.$0^{5,9}$.$0^{3,11}$] dodecane for explosives and propellants. PCT Int. Appl. WO 9720,785 (CI CO 61325134); 1995.
[50] Rao S, Reddy D, Rajagopal D. Process improvements in HNIW manufacture. In: Proceedings of the 31st international annual conference of ICT, Karlsruhe; 2000. p. 108/1–4.
[51] Shaohua J, Qinghai S, Shusen C, Yanshan S. Preparation of ε-HNIW by a One-pot method in concentrated nitric acid from tetraacetyldiformylhexaazaisowurtzitane. Propell Explos Pyrot 2007; 32(6):468–71.
[52] Nielson AT, Chafin AP, Christian SL. Synthesis of polyazapolycyclic caged polynitramines. Tetrahedron 1998;54(39):11793–812.
[53] Wang C, Ou Y, Chen B. One pot synthesis of hexanitrohexaazaisowurtzitane. Beijing Ligong Daxue Xuebao 2000; 20(4):521–3.
[54] Kawabe S, Miya H, Kodama T, Miyake N. Process for the preparation of hexanitrohexaazaisowurtzitanes. PCT International Application No. WO 980566 A1; 1998.
[55] Sanderson AJ, Warner KF, Wardle RB. Process of making 2,4,6,8,10,12-hexanitro-2,4,6,8,10,12-hexaazatetracyclo (5.5.0.$0^{5,9}$.$0^{3,11}$)-dodecane. PCT International Application No. WO2000052011 A2; 2000.
[56] Bayat Y, Zarandi M. Preparation of hexanitrohexaazaisowurtzitane (HNIW) nano particle by normal micro emulsion based nonionic surfactant. Int J Nanosci Nanotechnol 2013;9(3):115–20.
[57] Kodama T. Preparation of hexakis (trimethylsilylethylcarbamyl) hexaazaisowurtzitane. JP Patent 06321962 A2; 1994.
[58] Hamilton RS, Sanderson AJ, Wardle RB, Warner KF. Studies of the synthesis and crystallization of HNIW. In: Proceedings of the 31st international annual conference of ICT, Karlsruhe, Germany; 2000.
[59] Bayat Y, Mokhtari J. Preparation of 2,4,6,8,10,12-hexanitro-2,4,6,8,10,12-hexaazaisowurtzitane from 2,6,8,12-tetraacetyl 2,4,6,8,12-hexaazaisowurtzitane using various nitrating agents. Def Sci J 2011; 61(2):171–3.
[60] Chung HY, Kil HS, Choi I. New precursors for hexanitrohexaazaisowurtzitane (HNIW, CL-20). J Heterocyclic Chem 2000;37(6):1647–9.
[61] Ghosh M, Venkatesan V, Sidker AK, Sidker N. Preparation and characterization of ε-CL-20 by solvent evaporation and precipitation methods. Def Sci J 2012;62(6):390–8.
[62] Zhao X, Feng Z, Liu J. Preparation of high purity and high yield of HNIW from tetraacetylhexaazaisowurtzitane. In: Proceedings of the 33rd international annual conference of ICT, Karlsruhe; 2002. p. 149/1.
[63] Foltz MF, Coon CL, Gracia F, Nochols AL. The thermal stability of the polymorphs of hexanitrohexaazaisowurtzitane, part-I. Propell Explos Pyrot 1994;19:19–25.
[64] Gump JC, Peiris SM. Phase transitions and isothermal equations of state of epsilon hexaazaisowurtzitane (CL-20). J Appl Phys 2008;104:083509/1–4.
[65] Torry S, Cunliffe A. Polymorphism and solubility of CL-20 in plasticizers and polymers. In: Proceedings of the 31st international annual conference of ICT, Karlshure; 2000. p. 107/1–12.
[66] Tian Q, Yan G, Sun G, Huang C, Xie L, Chen B, et al. Thermally induced damage in hexanitrohexaazaisowurtzitane. Cent Eur J Energ Mater 2013;10(3):359–69.
[67] Zhang P, Xu J, Guo X, Jiao Q, Zhang J. Effect of addictives on polymorphic transition of ε-CL-20 in castable systems. J Therm Anal Calorim 2014;117:1001–8.
[68] Yang R, Xiao H. Dissociation mechanism of HNIW ions investigated by chemical ionization and electron impact mass spectroscopy. Propell Explos Pyrot 2006;31(2):148–54.
[69] Doyle RJ. The gas-phase dissociation of a new polyazapolycyclic nitramine: hexanitrohexaazaisowurtzitane. J Mass Spectrom 1991; 26:723–6.
[70] Pace MD. EPR spectra of photochemical nitrogen dioxide formation in monocyclic nitramines and hexanitrohexaazaisowurtzitane. J Phys Chem 1991;95(15):5858–64.
[71] Okovytyy S, Kholod Y, Quasim M, Fredrickson H, Leszynski J. The mechanism of unimolecular decomposition of 2,4,6,8,10,12-hexanitro-2,4,6,8,10,12-hexaazisowurtzitane, a computational DFT study. J Phys Chem A 2005;109(12):2964–70.
[72] Ryzhkov LR, McBride JM. Low-temperature reaction in single crystals of two polymorphs of the polycyclic nitramine ^{15}N-HNIW. J Phys Chem 1996;100(1):163–9.
[73] Patil DG, Brill TB. Thermal decomposition of energetic materials 59. Characterization of the Residue of hexanitrohexaazaisowurtzitane. Combust Flame 1993;92(4):456–8.
[74] Naik NH, Gore GM, Gandhe BR, Sidker AK. Studies on thermal decomposition mechanism of CL-20 by pyrolysis gas chromatography–mass spectrometry (Py-GC/MS). J Hazard Mater 2008;159:630–5.
[75] Valcovik V, Sudac D, Obhodas J, Eleon C, Perot B, Carasco C, et al. The use of alpha particle tagged neutrons for the inspection of objects on the sea floor for the presence of explosives. Nucl Instrum Methods Phys Res A 2013;703:133–7.
[76] Elbeih A, Husarova A, Zeman S. Path to ε-HNIW with reduced impact sensitivity. Cent Eur J Energ Mater 2011;8(3):173–82.
[77] Zeman S, Krupka M. New aspect of impact reactivity of polynitro compounds, Part-III. Impact sensitivity as a function of the intermolecular interactions. Propell Explos Pyrot 2003;28(6):301–7.
[78] Jungova M, Zeman S, Yan QL. Recent advances in the study of the initiation of nitramines by impact using their ^{15}N NMR chemical shifts. Cent Eur J Energ Mater 2014;11(3):383–93.
[79] Chen H, Li L, Chen S, Chen S, Jiao Q. Effect of additives on ε-HNIW crystal morphology and impact sensitivity. Propell Explos Pyrot 2012; 37:77–82.
[80] Sivabalan R, Gore GM, Nair UR, Saikia A, Venugopalan S, Gandhe BR. Study on ultrasound assisted precipitation of CL-20 and its effect on morphology and sensitivity. J Hazard Mater 2007;139(2):199–203.
[81] Chen H, Chen S, Lui J, If L, Jin S, Shi Y. Preparation of the spheroidized HNIW crystal. C.N. Patent 101624394, A 20100113; 2010.
[82] Doo KB. Spherical high density 2,4,6,8,10,12-Hexanitrohexaazaisowurtzitane and preparation thereof. K.R. Patent 224043 B1, Dong Woon Speciality Chemical Co., Ltd., South Korea; 1999.
[83] Elbieh AIM, Husarova A, Zeman S. Method of preparation of Epsilon- 2,4,6,8,10,12-Hexanitro-2,4,6,8,10,12-hexaazaisowurtzitane with reduced impact sensitivity. U.S. Patent 9,227,981 B2; 2016.
[84] Pelikan V, Zeman S, Yan QL, Erben M, Elbeih A, Akstein Z. Concerning the shock sensitivity of cyclo nitramines incorporated into a polyisobutylene matrix. Cent Eur J Energ Mater 2014;11(2):219–35.
[85] Li J, Brill TB. Nanostructured energetic composites of CL-20 and binders synthesized by sol gel methods. Propell Explos Pyrot 2006;31(1):61–9.
[86] Vail SL, Moran CM, Barker RH. The formation of N,N'-dihydroxyethylenebisamides from glyoxal and selected amides. J Org Chem 1965;30:1195–9.
[87] Gilbert EE. Tetramido derivatives of glyoxal. J Chem Eng Data 1974;19(2):182–3.
[88] Boyer JH, Ramakrishnan VT, Vedachalam M. 4,10-Dinitro-2,6,8,12-tetraoxa-4,10-diazatetracyclo[5.5.0.$0^{5,9}0^{3,11}$]dodecane. Heterocycles 1990;31:479–80.